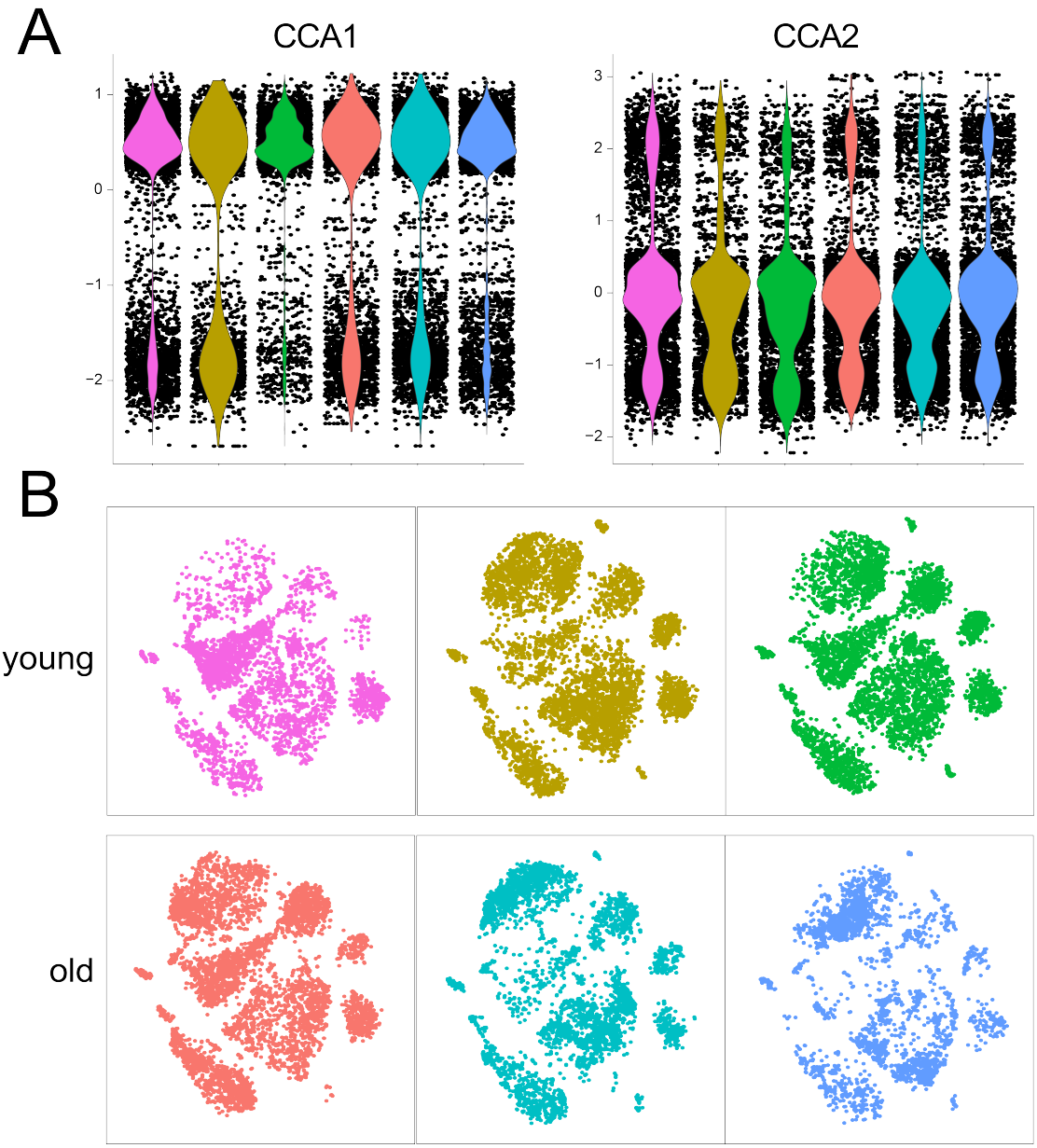

Supplemental Figure 1: Alignment of all samples. All 6 samples from young and old mice were aligned together in order to allow for inter-sample comparisons. (**A**) A canonical correlation analysis (CCA) was applied to identify common sources of variation between the datasets; the top 1000 variable genes of all samples were used to align the CCA subspaces of all samples in a new dimensional reduction (cca.aligned). (**B**) Using these aligned dimensions; it was possible to run a single integrated analysis on all cells. t-SNE plots show a complete overlap of all samples and no library preparation or sequencing batch effects.

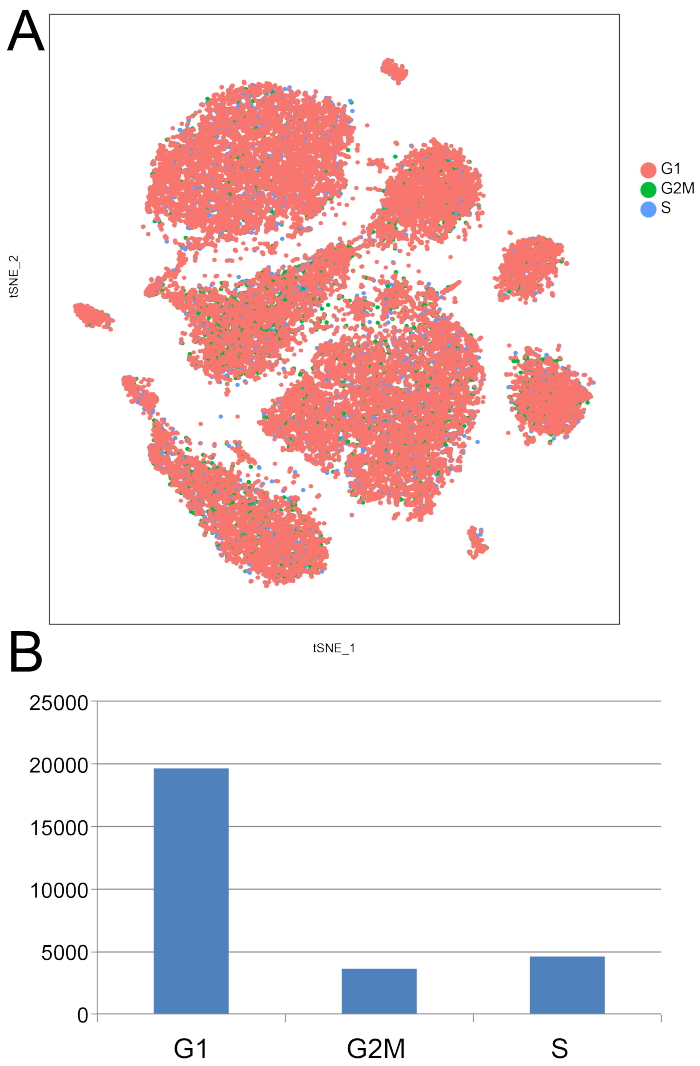

Supplemental Figure 2: (A) Quality control. Cell cycle distribution of all cells was predicted using mouse-trained model (see Materials and Methods). (**B**) t-SNE colored by cell stage. This quality control shows that data was homogeneous. Most of the cells were synchronized in G1 phase.

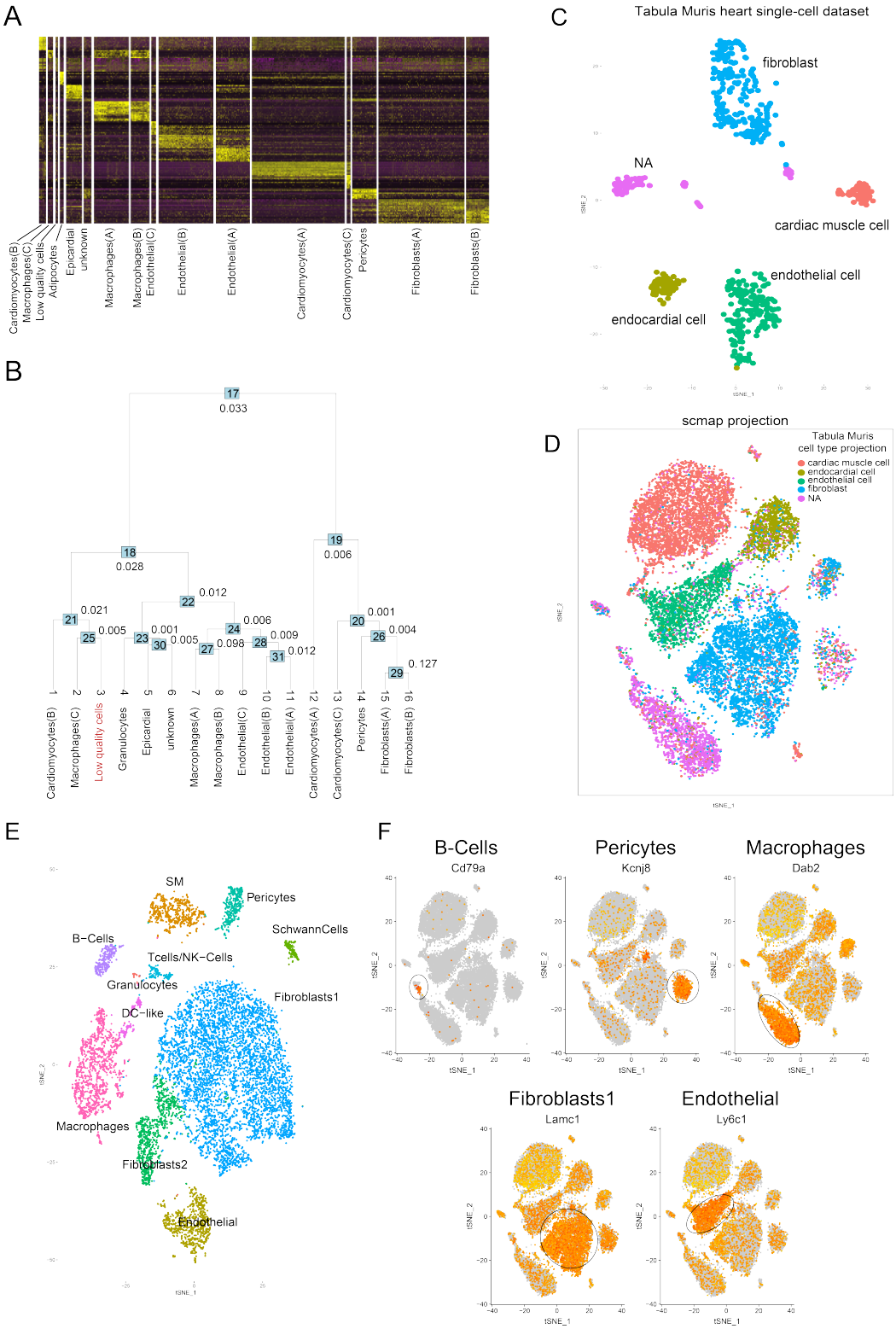

Supplemental Figure 3: (**A**) **Cluster analysis**. Genes enriched in each cluster were identified using a "ROC" test in Seurat (see Supplemental Table 2), comparing cells assigned to each cluster to all other cells. A heat-map was constructed using these genes found to define each cluster. The cluster labeled as "Low quality cells" in red showed excessive enrichment of mitochondrial genes; this one was not considered in further analysis as these nuclei likely represented low quality or dying cells. (**B**) We built a phylogenetic tree based on the distance matrix in gene expression of each cluster and we computed an out of bag error for each internal node of the tree. All

values below 0.1 show a high confidence for all clusters. Of note, fibroblasts A and B are within this threshold, so that these two different cell clusters can be separated with less confidence. (**C**) Heart cell type annotation derived from data of the Tabula Muris consortium (see Materials and Methods). (**D**) Projection of these RNA expression profiles to our single-nuclei RNA expression data. According to Tabula Muris consortium data, our endothelial A cluster should be considered endocardial cells. Cardiomyocyte B cells represent a merged cell type between endothelial cells and cardiomyocytes. Of note, cardiomyocytes may contain more than one nucleus, potentially in different states, which may complicate the assignment of such multinuclear cell types. In general, Tabula Muris data do not comprise many of our cell populations resulting in unidentified cells or cells with mixed signals, as was the case for pericytes, neuronal like cells and immune cells. (**E**) Heart cell type annotation derived from alternative single-cell heart data of Daniel et al. 2018 (see Materials and Methods). (**F**) Expressed gene markers of main cell types described in Daniel et al. 2018 in our cell populations (see Materials and Methods).

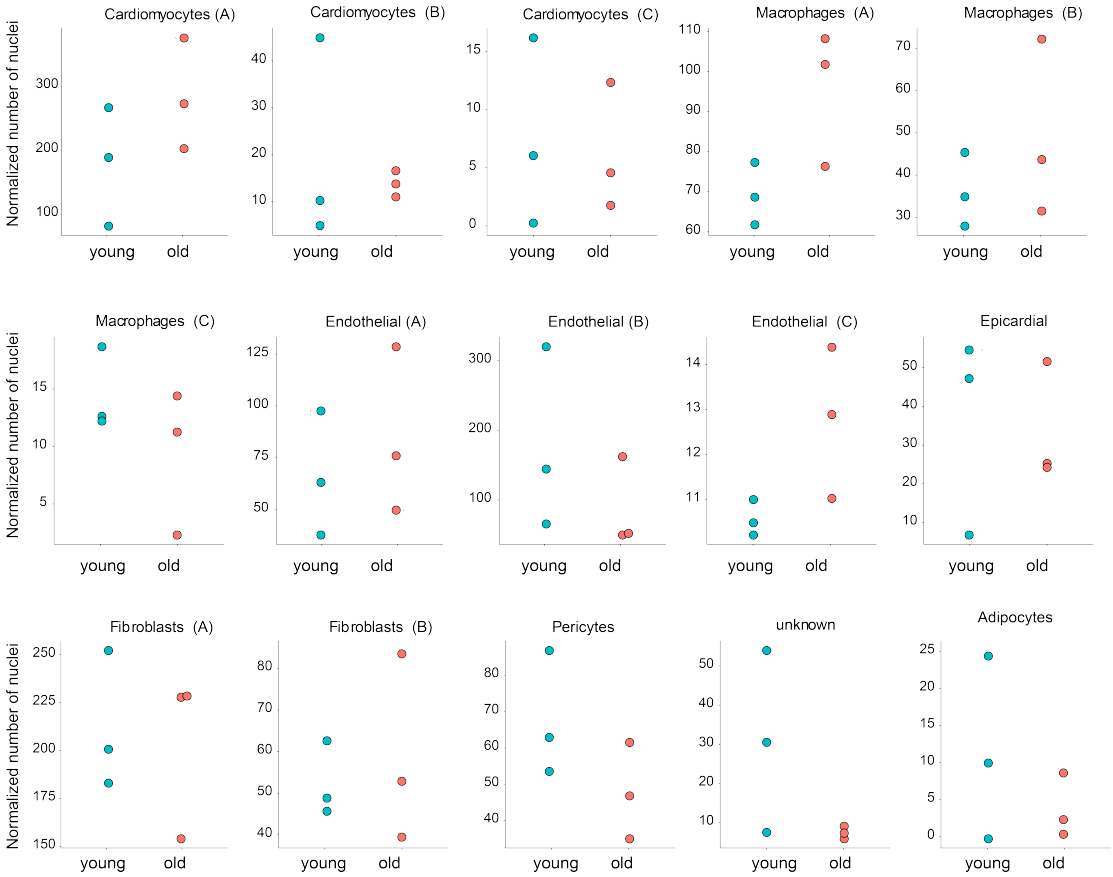

Supplemental Figure 4: Cell numbers. Comparison of number of nuclei on each cluster (normalized per 1000) between young and old samples detected by single-nucleus RNA-sequencing. In line with expectations we observed in particular for (multinucleate) cardiomyocyte A cells a trend for higher numbers of nuclei in old versus young samples. Due to too few numbers of samples, no statistical test could be reasonably applied to test potential mean differences significances. Although we observed some trends we do not have statistical power to find any significant change in cell (nuclei) population numbers.

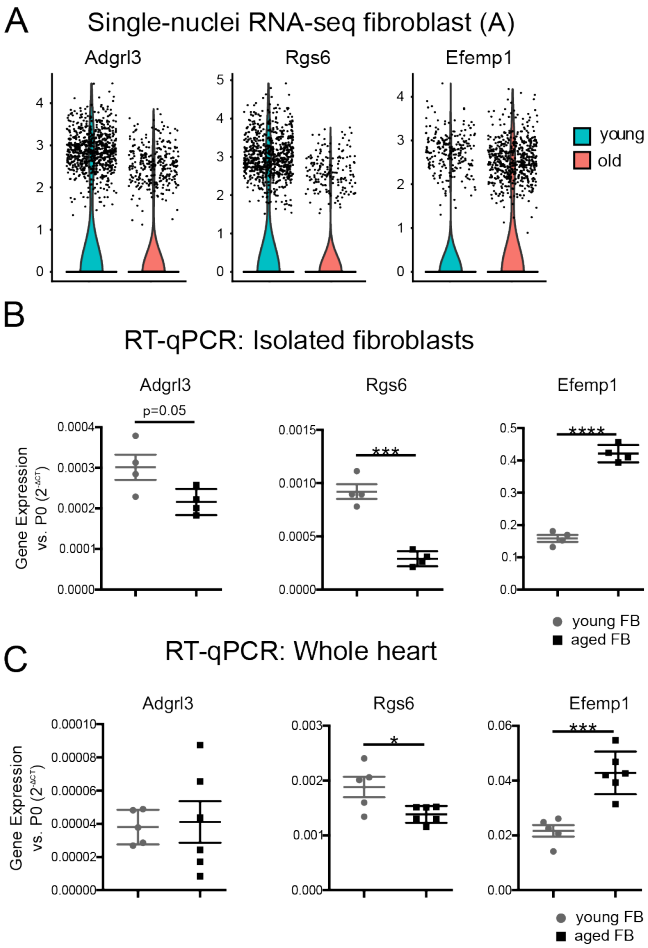

Supplemental Figure 5. Validation of fibroblast genes regulated by aging. (**A**) Violin plots of Adgrl3, Rgs6 and Efemp1 expressed in fibroblast population A derived from the single-nucleus sequencing data set. The validation of these genes was done via RT-qPCR with RNA derived from isolated cardiac fibroblasts (**B**) and RNA derived from whole mouse hearts (**C**). Data are shown as mean ± SEM (**B**, **C**). Statistical analysis was performed using the unpaired, two-sided T-test (**B**, **C**), indicated as follows: *P<0.05; ***P<0.001 and ****P<0.0001.

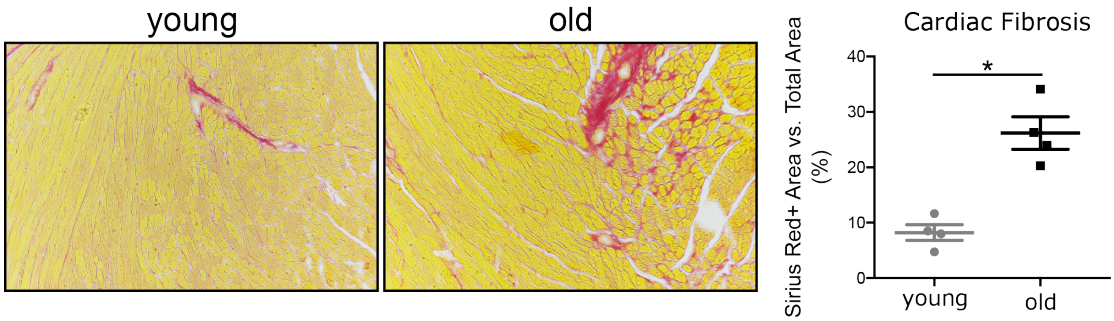

Supplemental Figure 6: Fibrosis in aged mice hearts. Fibrosis was determined via picrosirius red staining of young (12 weeks) and aged (20 months) mouse heart sections. Shown are 2 representative images of 24 images (n=4). Images were monitored using the Nikon Eclipse Ci microscope system and fibrosis was determined using the imageJ software. Data are shown as mean ± SEM. Statistical analysis was performed using the unpaired, two-sided T-test, indicated as follows: *P<0.05.

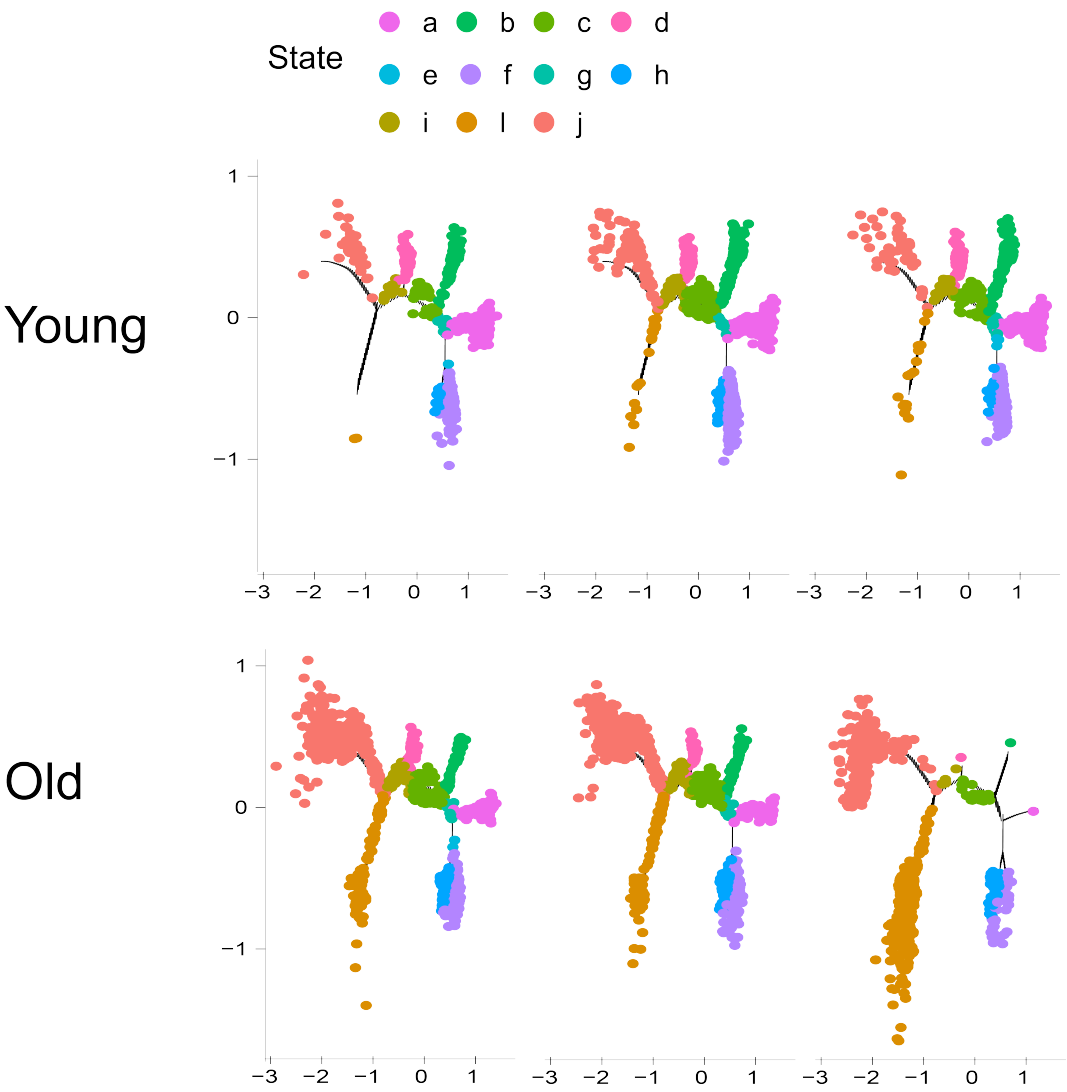

Supplemental Figure 7: Fibroblasts cell states in young and old mouse hearts. Samples feature a very similar cell state profile, showing data reproducibility. States are represented by different colours, enriched genes on each state is described in Supplemental Table 7. Each state can aggregate one or more fibroblast sub-cluster as shown in Figure 3B.

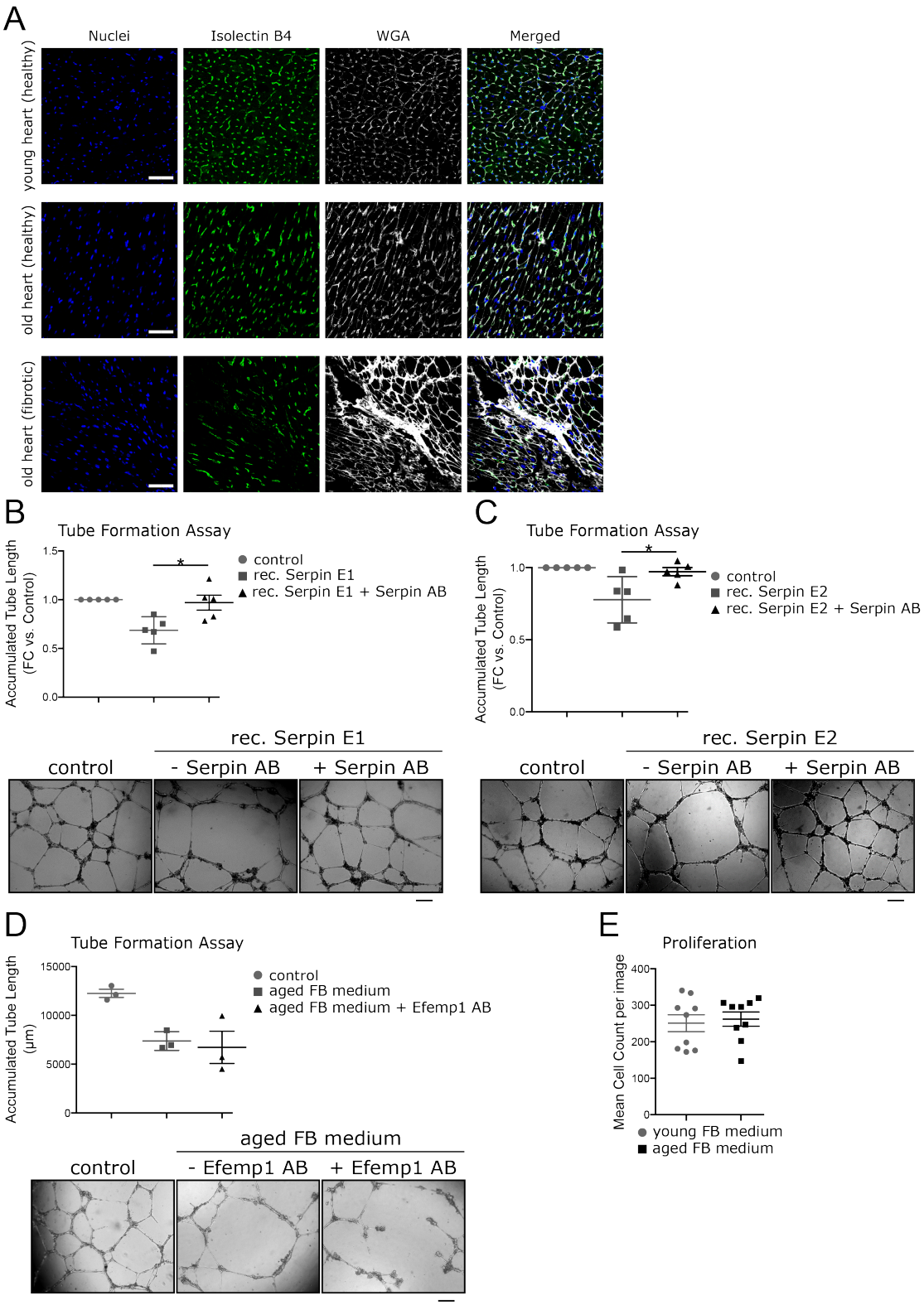

Supplemental Figure 8. Effect of fibroblast secretome on endothelial cells. (A) Capillary density of healthy young and healthy old, as well as fibrotic old heart sections. Capillaries were stained isolectin b4 (green), cell membranes with WGA (white) and nuclei (blue) with Hoechst 33342 (scale bar: 50 µm). (B) Tube formation assay of human umbilical vein endothelial cells (HUVEC) that were cultured in medium without any supplements (control), 10 ng/mL recombinant Serpin E1 (rec.

Serpin E1) or 10 ng/mL recombinant Serpin E1 + 4 µg anti-serpin antibody (rec. Serpin E1 + Serpin AB). Accumulated tube length was measured in five randomly chosen microscopic fields with a computer-assisted microscope using Axiovision 4.5 (Zeiss) (scale bar: 200 µm; n=5). (C) Tube formation assay. HUVECs that were cultured in medium without any supplements (control), 10 ng/mL recombinant Serpin E2 (rec. Serpin E2) or 10 ng/mL recombinant serpin E2 + 4 µg anti-serpin antibody (rec. Serpin E2 + Serpin AB). Accumulated tube length was measured in five randomly chosen microscopic fields with a computer-assisted microscope using Axiovision 4.5 (Zeiss) (scale bar: 200 µm; n=5). (D) Tube formation assay of HUVECs that were cultured in conditioned medium received from young (12 weeks) and aged (20 months) cardiac mouse fibroblasts. The aged phenotype was rescued by supplementing the aged fibroblast medium with 4 µg of an anti-Efemp1 antibody Accumulated tube length was measured in five randomly chosen microscopic fields with a computer-assisted microscope using Axiovision 4.5 (Zeiss) (n=3). (E) Proliferation of HUVECs cultured with conditioned medium received from young (12 weeks) and aged (18 months) cardiac mouse fibroblasts (n=9). Data are shown as mean ± SEM. Statistical analysis was performed using an unpaired, two-sided T-test, indicated as follows: *P<0.05.

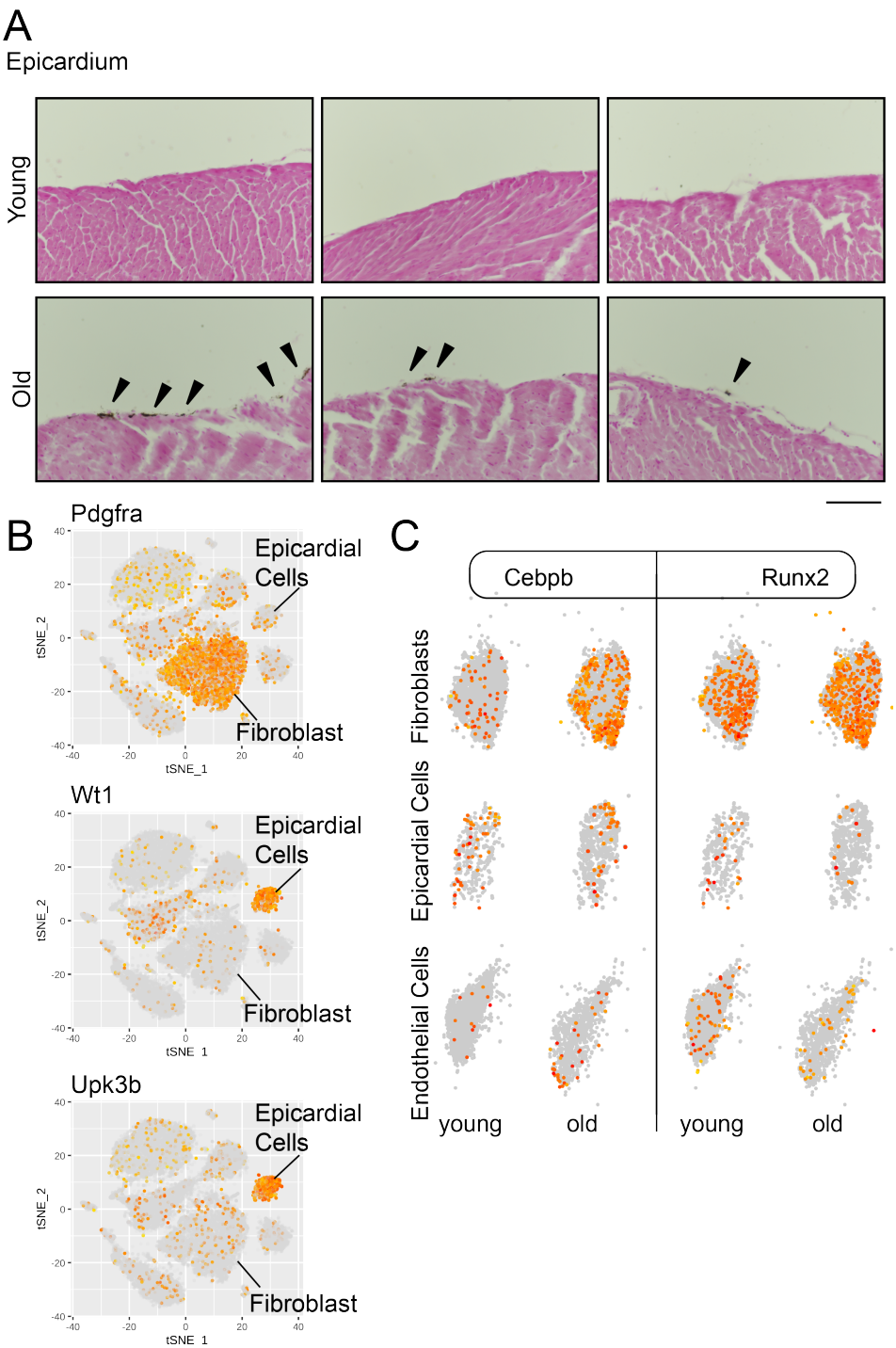

Supplemental Figure 9: Calcification in the aged epicardium. (A) Exemplary images of the epicardium in young (12 weeks) and old (20 months) mouse hearts. Calcification (dark spots, indicated by black arrows) is stained using the von Kossa staining method, whereas nuclei are stained with Kernechtrot (scale = 100 µm). (B)Expression of Pdgfra, Wt1 and Upk3b in young versus old nuclei cluster of the entire snRNA seq data set as shown in Figure 1A. (C) Expression of the osteogenic marker genes Cebpb and Runx2 in young versus old endothelial cell, fibroblast and epicardial cell clusters

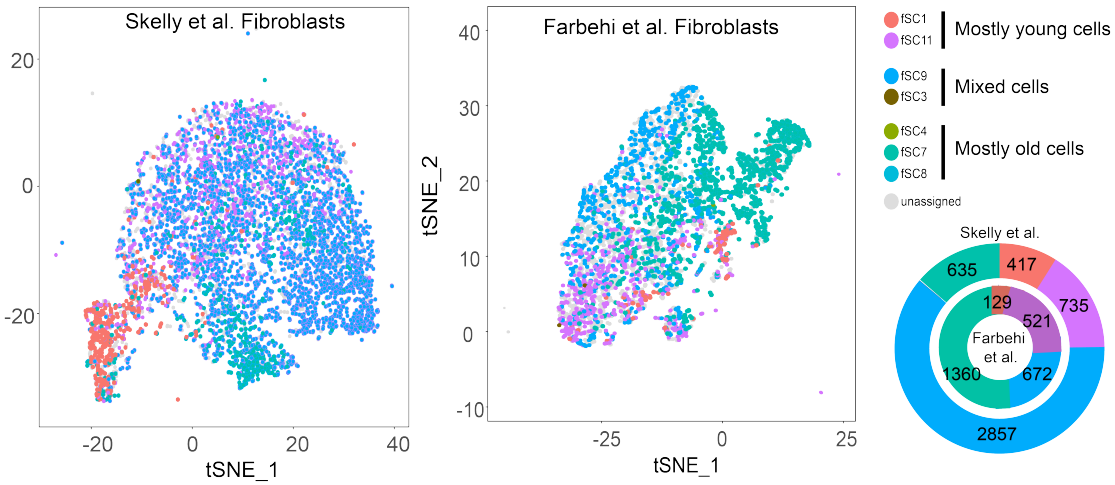

Supplemental Figure 10: Comparison of transcriptional profile from published fibroblast data. Using scmap (see methods), we mapped the fibroblast sub-cluster transcriptional profiles into already published datasets.

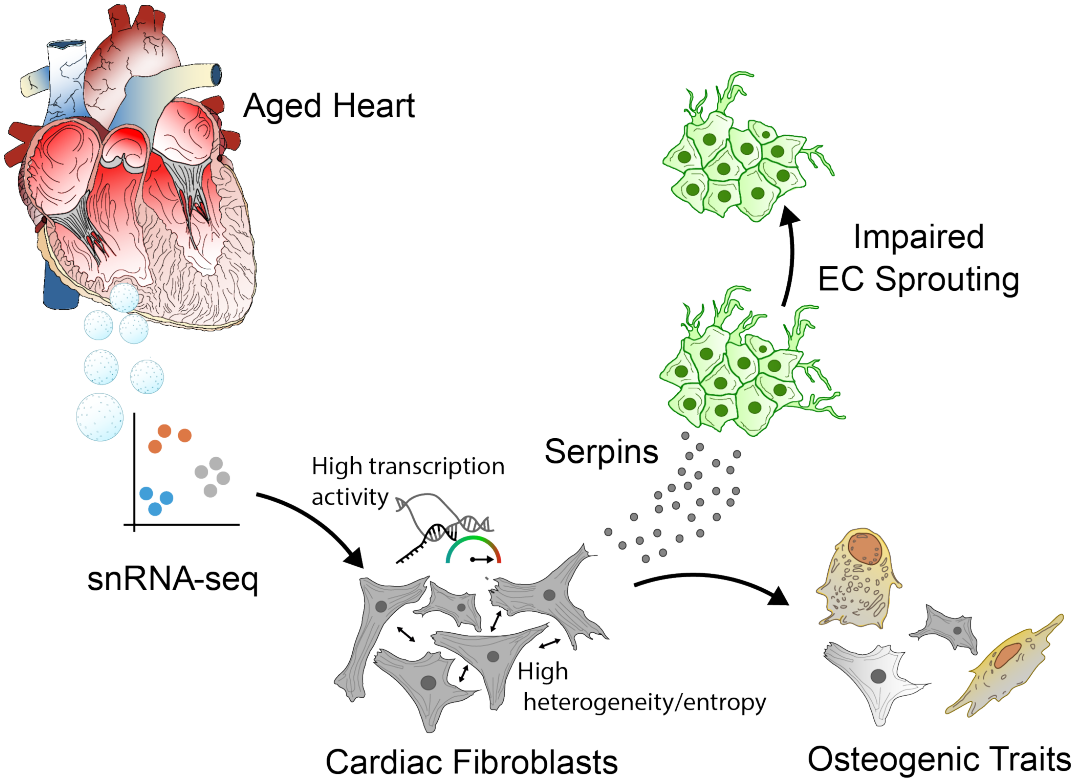

Supplemental Figure 11. Summary visual description of the aging heart by single cell analysis.